EasyChair Preprint

№ 8286

Improvement of Performance of Actuator with Adjustable Stiffness (AwAS) by Changing the Structure of the Mechanism and Using Sliding Mode Control Methodology

Hassan Mohammadi, Habib Ahmadi and Hamid Aris

June 18, 2022

Improvement of performance of Actuator with Adjustable Stiffness (AwAS) by changing the structure of the mechanism and using sliding mode control methodology

Hassan Mohammadi
Faculty of Mechanical Engineering
Babol Noshirvani University of Technology
Babol, Iran
hassan136984@gmail.com

Habib Ahmadi
Faculty of Mechanical and Mechatronics Engineering
Shahrood University of Technology
Shahrood, Iran
habibahmadif@shahroodut.ac.ir

Hamid Aris
Faculty of Mechanical and Mechatronics Engineering
Shahrood University of Technology
Shahrood, Iran
hamid.aris@shahroodut.ac.ir

***Abstract*— In recent years, due to the difficulty of rehabilitation exercises, rehabilitation robots have been used to assist physiotherapists, and due to the many interactions between the patient and the robot, robot safety is one of the most critical issues related to rehabilitation robots. In this paper, the mechanism of a variable stiffness actuator called AwAS is improved. Variable stiffness actuators are used in robots that have a lot of physical interactions with humans. The AwAS actuator has two motors. The first one controls the position and the second one controls the stiffness. The stiffness of the AwAS actuator is changed by changing the position of the springs embedded in it. The AwAS mechanism is such that the force required to move the springs to change the stiffness is approximately perpendicular to the force produced by the springs, ie the direction of their change in length. If these two forces are precisely perpendicular, the force required to move the springs will be minimized. In this paper, by changing the mechanism, the two forces are always perpendicular and less force is needed to move the spring. In this system, a sliding mode control methodology is used to prevent the robot vibrations. The robot has three degrees of freedom, and the dynamics of the system indicate that the system is nonlinear and has three inputs and three outputs that affect each other; that is, they are coupled together. Therefore, a method is used that is used for MIMO systems.**

Keywords—Robot, Variable stiffness actuator, AwAS, Sliding mode, control, MIMO

In recent years, rehabilitation robots have played a significant role in helping patients recover after a stroke. Despite their many advantages, these robots have not yet been widely used, and the main reason is the inability of their prototypes to adapt to action and therefore, it makes the robot unsafe to interact with humans. To this end, researchers are looking for ways to increase the robot safety. Most of the research was looking for ways to prevent the robot from injure humans and many different designs based on variable stiffness actuator have been presented. Nengbing Zhou et al. used a variable stiffness mechanism to improve human gait performance by helping the hip joint [1]. In VSJ [2] the effective length of the plate springs using a four-link system have been changed. The system works in such a way that the actuators connected to the input links cause them to rotate and by changing the relative positions of the output links, the slider moves and changes the effective length of the spring and consequently its stiffness. The problem with this structure is that the stiffness at its minimum changes very fast and causes vibration. In [3], a VSA uses three springs to change its stiffness. Stiffness of the mechanism depends on the number of springs that are active during the operation of the mechanism and the stiffness changes with increasing or decreasing the number of these springs. In vsaUT-II [4], the technique of changing the ratio of the transition between the internal elastic elements and the actuator have been used. They simulate by altering the point of contact of the elastic element, the point of application of the external force and the point of the hinge. O. Manolo Flores et al. simulated wrist movements to aid in physiotherapy. Their rehabilitation mechanism uses a pneumatic variable stiffness actuator (pVSA) that controls the stiffness of the system [5]. In AwAS [6] the fixing point of the connection between the two springs and the output link have been changed. In this structure, two antagonistic springs are connected to the middle link on one side and to the output link on the other side, and the middle link is rigidly connected to the main joint motor. Sliding mode control methodology for nonlinear multi-input multi-output systems should be used to prevent system vibrations. In the mechanism proposed by [7] a mechanism that used a VSA in its structure for use on the ankle. The stiffness of this inverted slider-crank mechanism is adjusted based on the external load and joint angle. In [8], a human-inspired soft finger with dual-mode morphing enabled by variable stiffness mechanism, used a U-shape VSA on their fabricated soft finger. Using this mechanism, they solved the problem of compromising compliance and agility when increasing stiffness. Elif Hocaoglu et al. used nonlinear springs to design their variable stiffness actuation mechanism. This mechanism simultaneously controls the stiffness and position of the prosthetic hand [9]. In [10], Christophe Lecomte et al. used a VSA in the design of their proposed prosthetic leg, which uses a motor that wirelessly controls the stiffness of the system. This motor changes the stiffness of the mechanism by moving the support points on a leaf spring. Zhuo Ma et al. improved a mechanism that had variable stiffness to strengthen the lower limb [11]. In [12], Zhongyi Li et al. designed a variable stiffness

mechanism for upper limb rehabilitation. One of the advantages of their design is large range of stiffness changes. A Series-Elastic Manipulator with Passive Variable Stiffness for Legged Robots (SiMPLeR) [13] have been designed by Sajiv Shah et al. They designed a variable stiffness linear spring using a torsional springs and timing belts by changing the motor and joint distance. In [14], Bing Chen et al. developed a mechanism for knee rehabilitation. They used a disk-type torsion spring to design their VSA mechanism. Simon Lemerle et al. used nonlinear elastic elements in their proposed mechanism to control the stiffness of the system. This mechanism, which uses three motors to position and control stiffness, is used to simulate wrist movements [15]. In [16], Yixin Shao and colleagues used a linear torsion spring to design the VSA in their proposed mechanism. Their mechanism is able to change the width of stiffness changes from 0 to infinity.

.

I. AWAS: MECHANISM CONCEPT

In this system, a pair of antagonistic springs are used according to Figure 1 by moving them, the stiffness of the mechanism can be changed. The novelty of this design is that in all cases where the output link has been displaced, no change in size occurs in the springs during the displacement of them, which means that much less energy is used to change the stiffness of the mechanism. As a result, the motor required to change stiffness will be smaller and cost less. As shown in Figure 1, a pair of reciprocating springs connect the middle link related to the first motor to the output link. Thus the lever arm is equal to the distance between the center of rotation of the middle link and the connection point of the middle link and the spring. According to Figure 2, these springs are moved by a motor and by a ball screw along the middle link, and the length of the lever arm, and as a result, changes the stiffness of the mechanism.

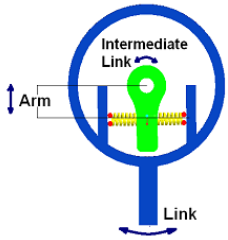

Figure 1 : AwAS-principle of operation

The total length of the two springs is always constant and therefore the pre-compression does not change during adjustment. In this model, the displacement that occurs to adjust the stiffness of the mechanism for the springs is perpendicular to the direction of the change in the length of the springs.

Also, during the movement of the springs along the middle link unlike the previous model, there is no size change in the springs, which means that the energy used to change this length will be eliminated. For this purpose, in the new design, the rods that are the means of the spring and the output link, using belt and pulleys, are always placed in parallel with the middle link.

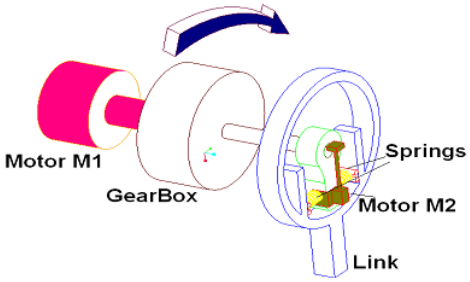

Figure 2. AwAS-conceptual design

As mentioned earlier, the existing mechanism has two separate motors. One is the M1 for movement, and the other is the M2 for adjusting the stiffness. The M1 is a DC motor with a torque peak of 2.35Nmn. As shown in Figure 2, it is connected to the middle link by a gearbox with a 50: 1 ratio. The M2 motor is a DC motor mounted on the middle link. The rotational motion of this motor is converted to a linear motion by a ball screw.

The two springs are pre-compression 6 mm before connection. The two linear guides attached to the output link guide the spring to move along the ball screw. The rods that mediate the spring and the output link (links 1 and 2) are connected to the M2 motor by Belt and pulleys so that they are always parallel to the middle link. Two locks are installed on the device to restrict movement between -0.2 and 0.2 + radians. This motion is the relative motion between the middle link and the output link; and the middle link can move in the range of -120 and +120 degrees.

II. MODIFIED MECHANISM

According to Figure 3 and using the similarity theorem, it is proved that unlike the original mechanism, in the proposed mechanism, the change in length occurs evenly throughout the diameter of the spring.

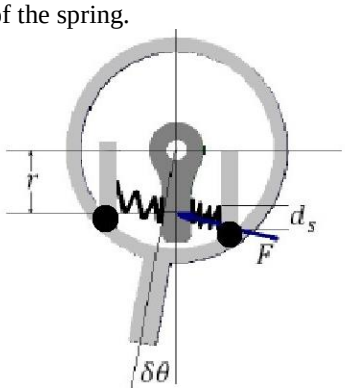

Figure 3. AwAS at an un-equilibrium position

Parameters in Fig3 represent:

Ks is the stiffness of each spring, δX is the change in the length of the springs, p2 is the pre-compression of the springs and Ds is the length of the middle link.

$$r+\frac{Ds}{2}<\tilde{r}<r+\frac{Ds}{2} \qquad (1)$$

The resultant force applied from the link to the springs is:

$$F = Ks\,(p2 + \delta X) - Ks\,(p2 - \delta X) = \quad (2)$$
$$2\,Ks\,\delta X = 2KsD_f \sin\delta\theta$$

The resultant torque can be calculated as:

$$T = F\tilde{r} \Rightarrow T = 2Ks\tilde{r}D_f \sin\partial\theta\cos\partial\theta \quad (3)$$

The total torque is equal to the sum of the torques produced by the entire spring diameter:

$$T = \frac{1}{Ds}\int_{r-Ds/2}^{r+Ds/2} 2Ks\tilde{r}D_f \sin\delta\theta\cos\delta\theta \quad (4)$$
$$= \frac{KsD_f \sin(2\delta\theta)}{Ds}\int_{r-Ds/2}^{r+Ds/2}\tilde{r} = rKsD_f \sin(2\delta\theta)$$

Hence the equivalent stiffness can be computed:

$$K = 2rKsD_f \cos(2\delta\theta) \quad (5)$$

In the new mechanism, the need to apply, the force required for this change in stiffness is eliminated. In the previous mechanism the force was:

$$F_{M2} = F\sin\delta\theta = 2Kr\sin^2\delta\theta \quad (6)$$

The energy required for this change in stiffness is eliminated in the new mechanism. This energy was:

$$E_{M2} = \int F_{M2}dr = Kr^2\sin^2\delta\theta \quad (7)$$

Essential parameters for fundamental changes in stiffness are equivalent stiffness (*Ks*) and arm length (r). The second motor changes r through ball screw. Θ_3 is the angle of rotation of the second motor. The relationship between Θ_3 and r is:

$$r = p\theta_3 \quad (8)$$

In this equation p equal the pitch of the ball screw.
The potential energy stored in the equivalent spring can be computed:

$$U_K = \frac{1}{2}K\delta\theta^2 \quad (9)$$

Also, if M_f is the mass and D_f is the length of the middle link, the potential energy resulting from the displacement of the output link can be calculated:

$$U_l = \frac{1}{2}M_l gD_l(1-\cos\theta_2) \quad (10)$$

Also, if M_f is the mass and D_f is the length of the middle link, the change of potential energy resulting from the displacement of the intermediate link is:

$$U_f = \frac{1}{2}M_f gD_f(1-\cos\theta_1) \quad (11)$$

The total potential energy is equal to the sum of the potential energies obtained.

$$U_T = U_f + U_l + U_K \quad (12)$$

If the moment of inertia of the middle link and the first motor are equal to I_f and I_{Ml}, respectively, the kinetic energy of the first motor and the middle link is:

$$T_f = \frac{1}{2}(I_{M_1} + I_f)\dot{\theta}_1^2 = \quad (13)$$
$$\frac{1}{2}\left(\frac{1}{2}m_1r_1^2 + \frac{1}{3}M_f D_f^{\,2}\right)\dot{\theta}_1^2$$

Also, if the moment of inertia of the output link is equal to I_L, the kinetic energy of the output link can be calculated:

$$T_L = \frac{1}{2}\left(\frac{1}{3}M_l D_l^{\,2}\right)\dot{\theta}_2^2 \quad (14)$$

The kinetic energy of the second motor is:

$$T_{M_3} = \frac{1}{2}\left(\frac{1}{2}M_2 r_2^2\right)\dot{\theta}_3^2 \quad (15)$$

The kinetic energy of the whole system is equal to the sum of the kinetic energies:

$$T_T = T_f + T_L + T_{M_2} \quad (16)$$

Lagrange equation is used to write the equation of motion:

$$\frac{d}{dt}\left(\frac{\partial L}{\partial\dot{q}_i}\right) - \frac{\partial L}{\partial q_i} = u_i \quad (17)$$
$$L = T - U$$

The system has three degrees of freedom, including Θ_1, Θ_2 and Θ_3. Θ_1 is the angle of rotation of the middle link and the first motor. Θ_1 is the output angle of the output link. Θ_1 is the angle of the second motor.
For $q_1=\Theta_1$, the equation of motion is:

$$\left(\frac{1}{2}m_1r_1^2 + \frac{1}{3}M_f D_f^{\,2}\right)\ddot{\theta}_1 - \quad (18)$$
$$2p\theta_3 KsD_f \sin(-2\theta_2 + 2\theta_1)(\theta_2 - \theta_1)^2$$
$$+\frac{1}{2}M_f gD_f \cdot\sin(\theta_1) -$$
$$2p\theta_3 KsD_f \cos(-2\theta_2 + 2\theta_1)(\theta_2 - \theta_1) = \mathrm{T1}$$

Also for $q_2=\Theta_2$, the equation of motion can be calculated:

$$\left(\frac{1}{3}M_L D_L^{\,2}\right)\ddot{\theta}_2 + \frac{1}{2}M_L D_L g\cdot\sin(\theta_2) \quad (19)$$
$$+2p\theta_3 KsD_f \sin(-2\theta_2 + 2\theta_1)(\theta_2 - \theta_1)^2 +$$
$$2p\theta_3 KsD_f \cos(-2\theta_2 + 2\theta_1)(\theta_2 - \theta_1) = T2$$

Finally, the equation of motion for $q_3=\Theta_3$ is:

$$\frac{1}{2}m_2r_2^{\,2}\ddot{\theta}_3 + \quad (20)$$
$$pKsD_f \cos(-2\theta_2 + 2\theta_1)(\theta_2 - \theta_1)^2 = T_3$$

Sliding control:
Θ_{1d}, Θ_{2d} and Θ_{3d} are desired angles:

$$\theta_{1d} = \left(\frac{45\pi}{180}\right)(1-\cos(2\pi t)) \quad (21)$$

$$\theta_{2d} = \left(\frac{55\pi}{180}\right)(1-\cos(2\pi t)) \quad (22)$$

$$\theta_{3d} = \left(\frac{65\pi}{180}\right)(1-\cos(2\pi t)) \quad (23)$$

The block diagram for sliding control is figure 4.

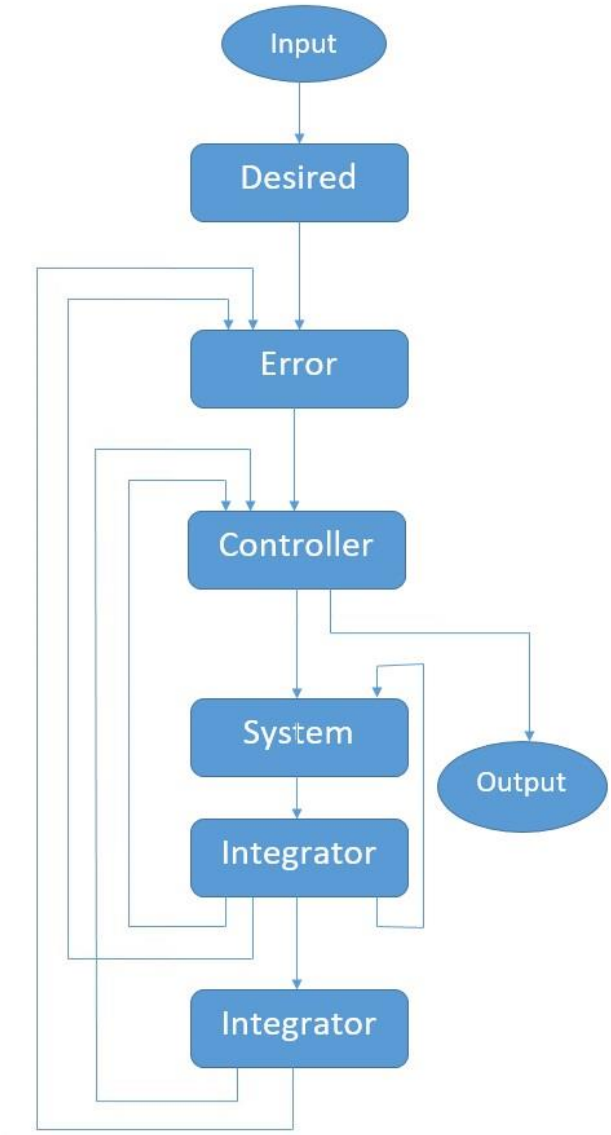

Figure 4 .View of simulation

$$\frac{1}{2}\frac{\partial}{\partial_t}S_i^{\,2} \le -\eta_i |S_i| \tag{24}$$

In this formula, s is the time-varying surface in the state-space and the ζ is a strictly positive constant.
S is defined as follows:

$$S = \dot{E} + \Lambda E = \dot{\theta} - \dot{\theta}_r \tag{25}$$

$$\dot{\theta}_r = \dot{\theta} - \Lambda E \tag{26}$$

In this formula, s is the sliding surface and ʌ is a strictly positive constant matrix, E is the system error rate. We define E and ʌ as follows:

$$\Lambda = \begin{bmatrix} 0.5 & 0 & 0 \\ 0 & 0.5 & 0 \\ 0 & 0 & 0.5 \end{bmatrix} \tag{27}$$

$$E = \begin{bmatrix} e_1 \\ e_2 \\ e_3 \end{bmatrix} \tag{28}$$

$$e_1 = \theta_1 - \theta_{1d} \tag{29}$$

$$e_2 = \theta_2 - \theta_{2d} \tag{30}$$

$$e_3 = \theta_3 - \theta_{3d} \tag{31}$$

$$\dot{\theta}_r = \begin{bmatrix} \dot{\theta}_{1d} \\ \dot{\theta}_{2d} \\ \dot{\theta}_{3d} \end{bmatrix} - \Lambda E \tag{32}$$

Θ_d is the desired angles of the system.
The Lyapunov function, which is a definite positive function, is defined as follows:

$$V = \frac{1}{2} S^T H S \tag{33}$$

According to the dynamics of the system and the solution of Lyapunov function, the robust control of the sliding mode is defined as follows.

$$\tau = \hat{\tau} - K\,\mathrm{sgn}(S) \tag{34}$$

The ζ is a 1 * 3 matrix, each of which is control input and the $\hat{\tau}$ is the best estimate of the equivalent control.
In this formula, the matrix K is control discontinuity and used to for parametric uncertainties:

$$K \ge \left|\hat{H}\ddot{q}_r + \hat{C} + \hat{D}\hat{G}\right| + \eta_i \tag{35}$$

where

$$K = \begin{bmatrix} k_1 & 0 & 0 \\ 0 & k_2 & 0 \\ 0 & 0 & k_3 \end{bmatrix} \tag{36}$$

Sliding mode control parameters are as follows:

$$\hat{\tau} = \hat{H}\ddot{q}_r + \hat{C} + \hat{D}\hat{G} \tag{37}$$

$$\tilde{H} = \hat{H} - H \tag{38}$$

$$\tilde{C} = \hat{C} - C \tag{39}$$

$$\tilde{G} = \hat{G} - G \tag{40}$$

$$\tilde{D} = \hat{D} - D \tag{41}$$

$$\tilde{H} = H * a \tag{42}$$

$$\tilde{C} = C * a \tag{43}$$

$$\tilde{G} = G * a \tag{44}$$

$$\tilde{D} = D * a \tag{45}$$

$$H = \begin{bmatrix} h_{11} & h_{12} & h_{13} \\ h_{21} & h_{22} & h_{23} \\ h_{31} & h_{32} & h_{33} \end{bmatrix} \tag{46}$$

$$H=\begin{bmatrix}0.0057 & 0 & 0\\ 0 & 0.0333 & 0\\ 0 & 0 & 0\end{bmatrix} \quad (47)$$

$$D=\begin{bmatrix}D_1 & 0 & 0\\ 0 & D_2 & 0\\ 0 & 0 & 0\end{bmatrix} \quad (48)$$

$$D_1=\frac{1}{2}*Mf*Df*sin(\theta_1) \quad (49)$$

$$D_2=\frac{1}{2}*ML*DL*sin(\theta_2) \quad (50)$$

$$c_{11}=-2*p*(\theta_3+0.05)*Ks*Df* \quad (51)$$
$$sin\left((-2*\theta_2)+(2*q1)\right)*(\theta_2-\theta_1)\wedge 2-$$
$$2*p*(\theta_3+0.05)*Ks*Df*$$
$$cos\left((-2*\theta_2)+(2*\theta_1)\right)*(\theta_2-\theta_1)$$

$$c_{22}=-c_{11} \quad (52)$$

$$c_{33}=p*Ks*Df* \quad (53)$$
$$cos\left((-2*\theta_2)+(2*\theta_1)\right)*(\theta_2-\theta_1)^2$$

$$G=\begin{bmatrix}g_1\\ g_2\\ g_3\end{bmatrix} \quad (54)$$

$$G=\begin{bmatrix}9.81\\ 9.81\\ 9.81\end{bmatrix} \quad (55)$$

a is another constant coefficient used to reduce system oscillations.

$$a=0.9885$$

In the above parameters h, c, d and g are the parameters of the system equations.

Thus the ζ matrix is obtained as follows.

$$\begin{bmatrix}\tau_1\\ \tau_2\\ \tau_3\end{bmatrix}=\begin{bmatrix}\hat{\tau}_1\\ \hat{\tau}_2\\ \hat{\tau}_3\end{bmatrix}-\begin{bmatrix}k_1 & 0 & 0\\ 0 & k_2 & 0\\ 0 & 0 & k_3\end{bmatrix}\mathrm{sgn}\left(\begin{bmatrix}s_1\\ s_2\\ s_3\end{bmatrix}\right) \quad (56)$$

Finally, the equations of the following system are controlled using the obtained controller.

$$\begin{bmatrix}\ddot{\theta}_1\\ \ddot{\theta}_2\\ \ddot{\theta}_3\end{bmatrix}=H^{-1}\left(\left(\begin{bmatrix}\tau_1\\ \tau_2\\ \tau_3\end{bmatrix}-\left(\begin{bmatrix}c_1\\ c_2\\ c_3\end{bmatrix}+\begin{bmatrix}D_1 & 0 & 0\\ 0 & D_2 & 0\\ 0 & 0 & D_3\end{bmatrix}\begin{bmatrix}g_1\\ g_2\\ g_3\end{bmatrix}\right)\right)\right) \quad (57)$$

$$\ddot{\theta}_i=H^{-1}\left(\tau_i-(C_i+D_iG_i)\right) \quad (58)$$

Figure 5 shows the result of tracking the three desired angles.

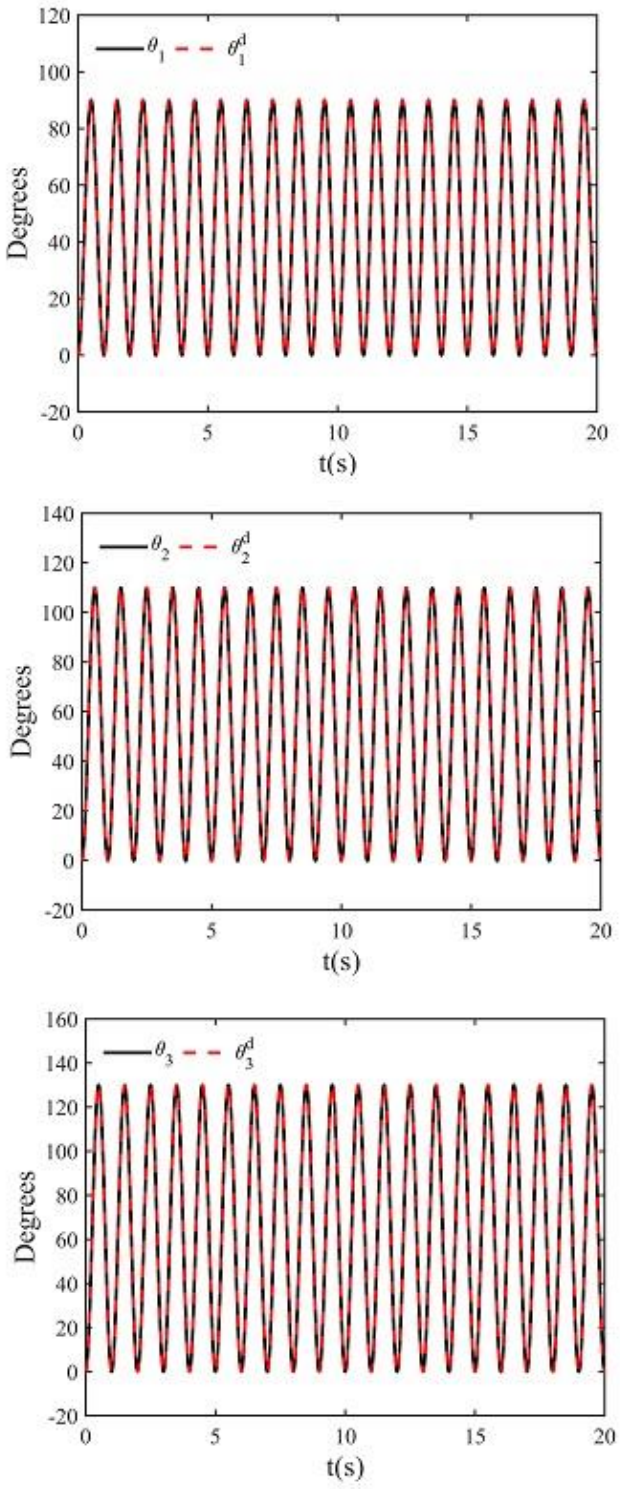

Figure 5. Tracking sine wave trajectory

Figure 6, which is related to the tracking error, shows that the error rate is negligible.

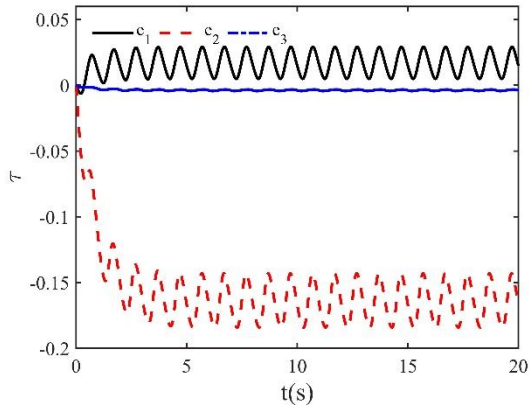

Figure 6. System tracking error

III. Conclusion

In this paper, the structure of a variable stiffness actuator called AwAS is improved. In the initial mechanism, two locks are used to bind the difference between the output link angle and the first motor. The reason for the present design is to reduce the energy consumption of the second motor. These constraints limit and weaken the mechanism. The energy required to change the stiffness increases exponentially in the absence of locks for greater angles. There is no such energy loss in the modified mechanism. As a result we can use a smaller motor as a second motor and reduce the cost. There is also no limit to the angle difference between the first motor and the output link. In addition to these benefits, you can use a ball screw with more steps. As a result, the stiffness adjustment speed increases. On the other hand, using the sliding mode control methodology, the tracking is done well, and the tracking error is negligible.

References

[1] Shao, Y., Zhang, W., Su, Y., & Ding, X. (2021). “Design and optimisation of load-adaptive actuator with variable stiffness for compact ankle exoskeleton”, In Mechanism and Machine Theory (Vol. 161, p. 104323). Elsevier BV.

[2] Choi, J., Park, S, Lee, W, & Kang, S. C, “Design of a robot joint with variable stiffness”, In Robotics and Automation, 2^08. ICRA 2008. IEEE International Conference on (pp. 1760-1765). IEEE.

[3] Hussain, I., Albalasie, A., Awad, M. I., Tamizi, K., Niu, Z., Seneviratne, L., & Gan, D. (2021). “Design and Control of a Discrete Variable Stiffness Actuator With Instant Stiffness Switch for Safe Human-Robot Interaction”, In IEEE Access (Vol. 9, pp. 118215–118231). Institute of Electrical and Electronics Engineers (IEEE).

[4] Groothuis S. S, Rusticelli, G, Zucchelli, A, Stramigioli, S and Carloni, R, “The vsaUT-II: A novel rotational variable stiffness actuator”, In Robotics and Automation (ICRA), 2012 IEEE International Conference on(pp. 3355-3360). IEEE.

[5] Flores, O. M., Lugo, J. H., Gonzalez, A., Maya, M., Gonzalez-Galvan, E. J., Zoppi, M., & Cardenas, A. (2021). “Design, Modeling, and Control of a Variable Stiffness Device for Wrist Rehabilitation”, In 2021 XXIII Robotics Mexican Congress (ComRob). 2021 XXIII Robotics Mexican Congress (ComRob). IEEE.

[6] Jafari, A, Tsagarakis, N. G, Vanderborght, B, and Caldwell, D. G, . “A novel actuator with adjustable stiffness (AwAS)”, In Intelligent robots and systems (iros), 2010 IEEE/rsj international conference on (pp. 4201-4206). IEEE.

[7] Shao, Y., Zhang, W., Su, Y., & Ding, X. (2021). “Design and optimisation of load-adaptive actuator with variable stiffness for compact ankle exoskeleton”, In Mechanism and Machine Theory (Vol. 161, p. 104323). Elsevier BV.

[8] Yan, J., Xu, Z., Shi, P., & Zhao, J. (2022). “A Human-Inspired Soft Finger with Dual-Mode Morphing Enabled by Variable Stiffness Mechanism”, In Soft Robotics (Vol. 9, Issue 2, pp. 399–411). Mary Ann Liebert Inc.

[9] Hocaoglu, E., & Patoglu, V. (2022). “Design, Implementation, and Evaluation of a Variable Stiffness Transradial Hand Prosthesis”, In Frontiers in Neurorobotics (Vol. 16). Frontiers Media SA.

[10] Lecomte, C., Ármannsdóttir, A. L., Starker, F., Tryggvason, H., Briem, K., & Brynjolfsson, S. (2021). “Variable stiffness foot design and validation”, In Journal of Biomechanics (Vol. 122, p. 110440). Elsevier BV.

[11] Ma, Z., Zuo, S., Chen, B., & Liu, J. (2021). “Friction Prediction and Validation of a Variable Stiffness Lower Limb Exosuit Based on Finite Element Analysis”, In Actuators (Vol. 10, Issue 7, p. 151). MDPI AG.

[12] Li, Z., Li, W., Chen, W.-H., Zhang, J., Wang, J., Fang, Z., & Yang, G. (2021). “Mechatronics design and testing of a cable-driven upper limb rehabilitation exoskeleton with variable stiffness”, In Review of Scientific Instruments (Vol. 92, Issue 2, p. 024101). AIP Publishing.

[13] Shah, S., & Saund, B. (2021). “SiMPLeR: A Series-Elastic Manipulator with Passive Variable Stiffness for Legged Robots”, In 2021 6th International Conference on Automation, Control and Robotics Engineering (CACRE). 2021 6th International Conference on Automation, Control and Robotics Engineering (CACRE). IEEE.

[14] Chen, B., Wang, B., Zheng, C., & Zi, B. (2021). “Design and Simulation of a Robotic Knee Exoskeleton with a Variable Stiffness Actuator for Gait Rehabilitation”, In 2021 27th International Conference on Mechatronics and Machine Vision in Practice (M2VIP). 2021 27th International Conference on Mechatronics and Machine Vision in Practice (M2VIP). IEEE.

[15] Lemerle, S., Catalano, M. G., Bicchi, A., & Grioli, G. (2021). “A Configurable Architecture for Two Degree-of-Freedom Variable Stiffness Actuators to Match the Compliant Behavior of Human Joints”, In Frontiers in Robotics and AI (Vol. 8). Frontiers Media SA.

[16] Shao, Y., Zhang, W., & Ding, X. (2021). “Configuration synthesis of variable stiffness mechanisms based on guide-bar mechanisms with length-adjustable links”, In Mechanism and Machine Theory (Vol. 156, p. 104153). Elsevier BV.